

Optics Letters

Study of gain efficiency in quasi-distributed amplification systems

O. V. SHTYRINA,* A. Y. KOKHANOVSKIY, I. A. YARUTKINA, A. S. SKIDIN, A. V. IVANENKO, S. A. EFREMOV, B. N. NYUSHKOV, S. V. SMIRNOV, AND M. P. FEDORUK

Novosibirsk State University, 2 Pirogova Street, Novosibirsk 630090, Russia

*Corresponding author: olya.shtyrina@gmail.com

Received 27 November 2019; accepted 11 December 2019; posted 16 December 2019 (Doc. ID 384206); published 10 January 2020

We propose the mathematical model of quasi-distributed gain in fiber laser systems with cavity dumping. Particularly, we consider in detail the case of a small number of periodic cells in such lasers. The study of the signal gain in Yb-doped active fiber includes the experimental measurement of its characteristics and the theoretical approximations based on experimental results. Theoretical analysis of laser schemes with quasi-distributed gain considered here enables optimization of the output pulse characteristics for various numbers of active fiber cells. © 2020 Optical Society of America

<https://doi.org/10.1364/OL.384206>

Fiber lasers with quasi-distributed gain enable generating high-energy pulses by combining several sections of active fiber [1]. In such lasers, high-output energy is achieved as a result of the long cavity length and multiple signal gains inside the laser cavity. However, to achieve high-output energies, it is necessary to optimize both the cavity device order and the set of laser parameters. To perform optimization, analytical studies are necessary. In this work, we consider a fiber laser setup that consists of several cells of active fibers, passive fibers, and optical devices that introduce additional losses. Such a scheme can be used to work with fiber lasers with quasi-distributed gain in the case of non-periodical cells and fiber lasers with cavity dumping [2–8] with strong periodic cells, as depicted in Fig. 1. Here we consider strong periodic cells. Since the number of laser parameters to be optimized grows with the number of active fiber cells, it is necessary to develop new effective theoretical approximations that make it easier to obtain the optimal laser parameters. In this Letter, we propose a general theoretical method to find the gain distribution in a fiber laser with quasi-distributed gain and study the behavior of the output signal for various parameters of a fiber laser with cavity dumping.

In order to simulate and optimize the average output power in fiber lasers with quasi-distributed gain, here we propose the theoretical method to estimate the small signal gain and saturation power as a function of experimental setup characteristics in a normal dispersion Yb-doped active fiber.

The measurement scheme of the Yb-doped fiber gain is shown in Fig. 2. We use a figure-eight fiber laser based on a

polarization-maintaining fiber as a source of input pulses [9]. The source provides short pulses with a duration of 40 ps at the repetition rate of 15.16 MHz. To vary average power of input pulses in the range of 0.0005–0.5 W, we use an additional fiber pre-amplifier. Amplified pulses are launched into measured amplifying double-clad fiber LIEKKI Yb 1200—6/125 with a length of 2.5 m. We consistently measure average power of output pulses for different pumping powers in the range of 0.2–3.6 W at 976 nm. The power of output pulses is measured by integrating an optical spectrum registered by an optical spectrum analyzer.

Normally, to measure the small signal gain of the input signal with power less than 0.1 μW, one needs to use additional devices (such as additional couplers) in the experimental scheme [10]. However, to estimate the properties of Yb fiber, we propose here the method of coefficient estimation, which does not need additional experiment measurements for the small input signal.

The Yb-doped fiber signal gain can be analytically described using the effective two-level gain model [11,12]. This model can be applied directly using the previously obtained analytical results [10]; however, the major drawback of this model is that it does not take into account the background losses, or it is not

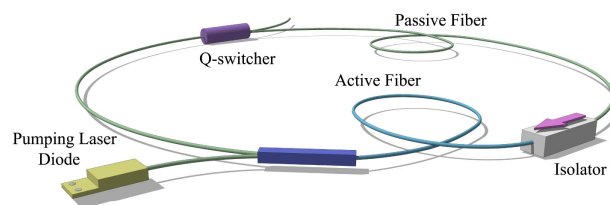


Fig. 1. Scheme of fiber laser with quasi-distributed gain.

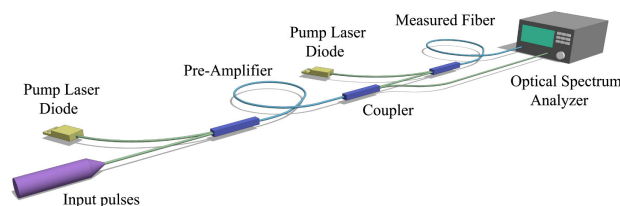


Fig. 2. Experimental measurement scheme.

integrable when including the background losses. Alternatively, the signal gain can be estimated numerically using the simple gain model based on the Schrödinger equation [13]. This model is used widely for the mathematical description of the signal evolution in all-normal ultra-long fiber lasers.

In the simple gain model, the saturation power and the small signal gain are functions of the pump power P_{pump} and fiber length L . In pulsed fiber lasers, the propagation of a signal in an active fiber is governed by the generalized nonlinear Schrödinger equation:

$$\frac{\partial A}{\partial z} = -i\frac{\beta_2}{2}\frac{\partial^2 A}{\partial t^2} - i\gamma|A|^2A + \frac{g/2}{1 + P(z)/P_{\text{sat}}}A - \frac{\alpha}{2}A. \quad (1)$$

Here β_2 and γ denote the dispersion and nonlinearity coefficients, respectively, g is the small signal gain coefficient, $P(z)$ is the average power at a given point inside the active fiber, P_{sat} is the gain saturation power, and α denotes the background losses.

To apply Eq. (1), it is necessary to know the saturation power P_{sat} and the small signal gain g . They can be derived theoretically from the gain coefficients measured experimentally for various input powers, pump powers, and active fiber lengths. In the theoretical method that we propose here, at first we estimate the small signal gain from the experimental results using the simple model based on Eq. (1) with $\alpha = 0$. After this, we estimate the value of P_{sat} using a more accurate model that takes into account background losses.

Let us examine the proposed algorithm in detail.

1. As a result of the experiment, we have the dependence of the signal gain $G = P(L)/P(0)$ on the input power $P(0)$. Here $P(L)$ is the signal power at the fiber output. Signal gain G is measured for different pump powers. Thus, $G = G(P_{\text{pump}}, P(0))$ is a function of the pump power P_{pump} and the input power. Similarly, the saturation power $P_{\text{sat}} = P_{\text{sat}}(P_{\text{pump}})$, and the small signal gain $g = g(P_{\text{pump}})$.

To estimate the background losses, an experiment for small fiber lengths and small pump powers was carried out; in this case, the coefficient $\alpha = 0.09 \text{ m}^{-1}$ was estimated using asymptotic signal gain for the large input signal, as shown in Ref. [10].

2. From the experiment, we have the values $G_i^j = G(P_{\text{pump}}^j, P_i(0))$ for P_{pump} from 0.3 W to 3.5 W. Here the upper index j corresponds to the j -th experimental curve, and the lower index corresponds to the i -th experimental point on the j -th curve. We consider here the experimental results for a fixed pump power. For each experiment, we obtain the small signal gain g using the signal gain G as follows: to determine the non-saturated gain, we use the simplified model without linear losses $P_z(z) = \hat{g}P(z)/(1 + P(z)/P_{\text{sat}})$. By integrating the simplified model, one can obtain the linear system of equations in order to estimate \hat{g} using the least-square method:

$$\forall P_{\text{pump}}^j : \sum_i \left(\frac{P_i(0)(G_i^j - 1)}{P_{\text{sat}}^j} + \ln G_i^j - \hat{g}^j L \right)^2 \rightarrow \min_{P_{\text{sat}}^j, \hat{g}^j}$$

The dependence of small signal gain on the pump power may be obtained by the minimization of this functional with respect to the unknown parameters (P_{sat}^j , \hat{g}^j),

$$g^j = g(P_{\text{pump}}^j) = \hat{g}^j + \alpha:$$

$$\hat{g}^j L = \frac{\left[\sum_i \Psi_i^j \right] \times \left[\sum_i \Psi_i^j \ln G_i^j \right] - \left[\sum_i (\Psi_i^j)^2 \right] \times \left[\sum_i \ln G_i^j \right]}{\left[\sum_i 1 \right] \times \left[\sum_i (\Psi_i^j)^2 \right] - \left[\sum_i \Psi_i^j \right]^2}, \quad (2)$$

where $\Psi_i^j = P_i(0)(G_i^j - 1)$, and $\sum_i 1$ is the number of points on the experimental curve. The corresponding theoretical approximation is shown in Fig. 3(a) by the dashed curve, and the dots correspond to the experimental data.

3. For each set of experimental results for a given P_{pump} , the theoretical small signal gain $g(P_{\text{pump}})$ has been obtained above; consequently, one can determine the saturation power as a function of the input signal power $P_{\text{sat}} = \hat{P}_{\text{sat}}(P(0), G)$ at each point on the experimental curve (using the full gain model with linear losses):

$$\frac{\hat{P}_{\text{sat}}(P(0), G)}{P(0)} = \frac{\alpha/g}{1 - \alpha/g} \times \frac{\exp((1 - \alpha/g)\alpha L)G - G^{\alpha/g}}{\exp((1 - \alpha/g)\alpha L) - G^{\alpha/g}}. \quad (3)$$

Using the least-square method and Eq. (3), one can obtain the average saturation power for each experimental curve:

$$\forall P_{\text{pump}}^j : P_{\text{sat}}^j \times \left[\sum_i P_i(0) / \hat{P}_{\text{sat}}(P_i(0), G_i^j) \right] = \left[\sum_i P_i(0) \right], \quad (4)$$

where $\hat{P}_{\text{sat}}(P_i(0), G_i^j)$ denotes the saturation power from Eq. (3) at the i -th point of the experimental curve that corresponds to a given P_{pump}^j .

Figure 3(b) demonstrates the dependence of the pump power on the saturation power: the dashed line shows the theoretical approximation, and the dots show the experimental data.

One can see that the experimental results in Fig. 3 can be approximated using the following formulas (P_{pump} is measured in W):

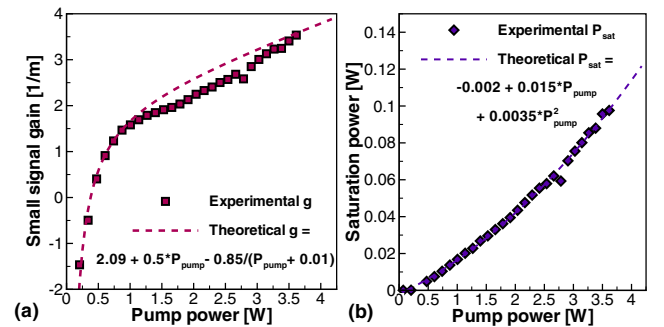


Fig. 3. Theoretical and experimental dependence of (a) small signal gain and (b) saturation power on the pump power. The dashed lines show the theoretical approximation, and the dots show the experimental data.

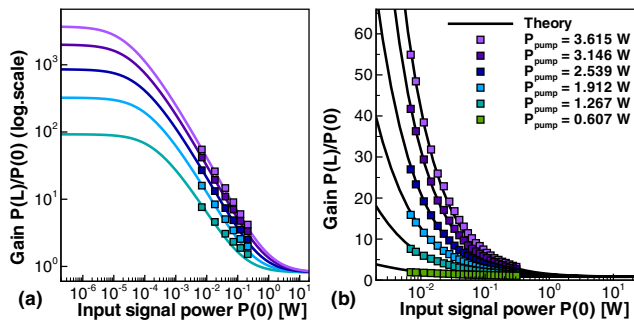


Fig. 4. Dependence of signal gain on the input signal power for different pump power values in (a) logarithmic scale and (b) natural scale. Dots correspond to the experimental results, and solid curves illustrate theoretical estimation.

$$g[1/m] = 2.09 + 0.5 \cdot P_{\text{pump}} - 0.85/(P_{\text{pump}} + 0.01),$$

$$P_{\text{sat}}[W] = -0.002 + 0.015 \cdot P_{\text{pump}} + 0.0035 \cdot P_{\text{pump}}^2.$$

Figure 4 shows the comparison of experimental (dots) and theoretical (solid curves) dependence of the signal gain on the input signal power for different experimental pump powers and chosen fiber length. As seen in the figure, theoretical approximation is in good accordance with the experimental results.

To study the dynamics of a slowly varied envelope in the fiber, we use the non-conservative nonlinear Schrödinger equation [Eq. (1)]. To obtain the generation regimes with a stable energy balance inside the laser cavity, we use the balance equations that describe the dynamics of the average power P inside the active medium:

$$\frac{\partial P(z)}{\partial z} = \left(\frac{g}{1 + P(z)/P_{\text{sat}}} - \alpha \right) P(z) \Rightarrow$$

$$\frac{P(0)}{P_{\text{sat}}} = \left(\frac{g}{\alpha} - 1 \right) \frac{C - G^{\alpha/g}}{CG - G^{\alpha/g}}, \quad C = \exp \left\{ \left(1 - \frac{\alpha}{g} \right) \alpha L \right\},$$

where $G = P(L)/P(0)$ is the saturated gain coefficient.

During the theoretical study, we have developed the general iterative method to find the gain distribution along the laser cavity. In order to estimate the intracavity dynamics of the average power, we consider the cavity with quasi-distributed gain as a ring cavity with n active fiber sections and multiplicative losses. In Fig. 1, n corresponds to the number of roundtrips of the active fiber during the roundtrip time T_R . On these assumptions, the average power dynamics depends only on the gain coefficients G_i ($1 < G_i < \exp\{(g - \alpha)L_i\}$) and coefficients of losses R_i ($R_1 = \dots = R_{n-1} \neq R_n = R_{n-1} \cdot R_{\text{out}} < 1$), where i denotes the number of the active fiber section, and L_i is the length of the i -th active fiber. Thus, the total gain is $G_{\text{total}} \equiv 1 / \prod R_i = \prod G_i$.

In general, we can use the set of coefficients $\{G_i^0 = (G_{\text{total}})^{1/n}, 1 \leq i \leq n\}$ as the initial gain distribution. For this configuration, the optimal initial distribution is the following: $\{G_i^0 = (q)^i / R_{n-1}; q = R_{\text{out}}^{-2/(n(n+1))}, 1 \leq i \leq n\}$. Here the upper index corresponds to the iteration number.

Thus, we obtain the following iterative process:

$$\left\{ P_i(0)^j = P_{\text{sat}} \left(\frac{g}{\alpha} - 1 \right) \left(C - (G_i^j)^{\alpha/g} \right) / \left(G_i^j C - (G_i^j)^{\alpha/g} \right) \right\} :$$

if $(P_i(0)^j G_i^j R_i < P_{i+1}(0)^j) \& (P_{i-1}(0)^j G_{i-1}^j R_{i-1} > P_i(0)^j) \Rightarrow$
the value of G_i^j is overestimated, then $G_i^{j+1} = G_i^j / (1 + \varepsilon_1)$;
if $(P_i(0)^j G_i^j R_i > P_{i+1}(0)^j) \& (P_{i-1}(0)^j G_{i-1}^j R_{i-1} < P_i(0)^j) \Rightarrow$
the value of G_i^j is underestimated, then $G_i^{j+1} = G_i^j \times (1 + \varepsilon_1)$;
else $\Rightarrow G_i^{j+1} = G_i^j; \quad 1 \leq i \leq n$.

We use the iteration process with the following convergence criterion: $\max_{1 \leq i \leq n} |P_i(0)^j G_i^j R_i - P_{i+1}(0)^j| / P_{i+1}(0)^j < \varepsilon_2$. In the iterative process, ε_1 and ε_2 are small preassigned values.

In the case of highly nonlinear intracavity dynamics, one can use a more general model that takes into account the dependence on the pump power and background losses in the active fiber [14–16]. This algorithm can be easily generalized due to the integrability of the effective two-level gain model.

Figure 5(a) shows the signal power dynamics in a laser cavity with eight active fiber sections for different output reflectivities on the Q -switcher R_{out} from 0.05 to 0.5. Here $g = 3.61/m$, $P_{\text{sat}} = 93$ mW, $\alpha = 0.091/m$, and $L = 2.5$ m for the pump power 3.5 W. The loss coefficients between active fibers R_1, R_2, \dots, R_{n-1} are equal to $\exp(-2 \cdot L_{\text{PF}} + 1) \cdot \ln(10)/10 \cdot R_S \approx 0.68$, and they include the passive fiber losses, 1 dB isolator losses, and pass switcher coefficient $R_S = 0.9$; the coefficient $R_n = R_{n-1} \cdot R_{\text{out}}$ additionally includes the output reflectivity on the Q -switcher. In Fig. 5(a), one can see that the signal gain in the n -th active fiber G_n approaches $1/R_{n-1}$ with the increase in n .

Figure 5(b) shows the dependence of output average signal power on the number of active fiber sections for different output reflectivities on the Q -switcher. It may be seen that the signal power has non-trivial behavior for a small number of fiber sections. At $n = 1$, there is an analytical solution represented as follows:

$$\frac{E_{\text{out}}}{T_R} = P_{\text{out}} = (1 - R_{\text{out}}) R_S \left(\frac{g}{\alpha} - 1 \right) \times \frac{P_{\text{sat}} \left(C - R_n^{-\alpha/g} \right)}{R_n^{-1} C - R_n^{-\alpha/g}}, \quad (5)$$

where roundtrip time $T_R = n_0 \cdot (L + L_{\text{PF}})/c$, c is the speed of light in vacuum, L_{PF} is the passive fiber length, and $n_0 \approx 1.5$ is the refractive index of the core. In Fig. 5(b), one can see that the output power P_{out} is inversely proportional to the number of fiber sections n ; thus, the further increase in number of sections

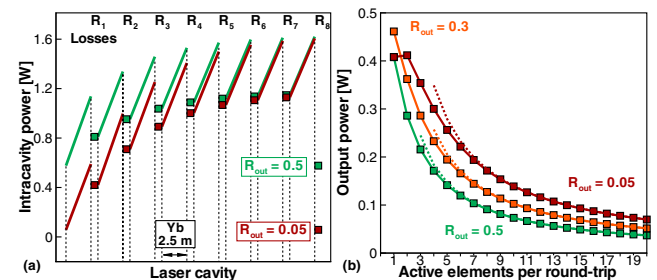


Fig. 5. (a) Signal power dynamics in laser cavity with eight active fiber sections; (b) dependence of the output average power on the number of active cavity elements. Dotted lines show similar theoretical dependencies corresponding to asymptotic behavior according to Eq. (6).

is not viable. Hence, the optimal output signal energy for the considered laser scheme is

$$\frac{E_{\text{out}}}{T_R} = P_{\text{out}} = (1 - R_{\text{out}}) \frac{R_S}{n} \left(\frac{g}{\alpha} - 1 \right) \times \frac{P_{\text{sat}} \left(C - R_{n-1}^{-\alpha/g} \right)}{R_{n-1}^{-1} C - R_{n-1}^{-\alpha/g}}, \quad (6)$$

where roundtrip time $T_R = n_0 \cdot \sum_{i=1}^n (L_i + L_{\text{PF}}) / c = n_0 \cdot (L + L_{\text{PF}}) \cdot n / c$. Figure 5(b) shows that Eq. (6) is applicable to the presented configuration with more than seven active elements.

As the theoretical analysis shows, in order to maximize the output energy in fiber lasers with distributed gain, one should minimize the losses inside the periodic section and maximize the output reflectivity.

We treat the gain efficiency as the ratio of the achieved output energy to the pump power needed to achieve such energy; in these terms, the use of cavity dumping allows to improve the gain efficiency. It is possible to further increase the output energy, because we have the almost unlimited possibility to compensate for the output losses on the Q -switcher. For a system with periodic amplification, the output energy is a linear function of the fiber section length. On the contrary, if the number of fiber sections is increased and the section length stays the same, the output energy tends to a constant value when the number of fiber sections grows indefinitely. Another advantage of the quasi-distributed gain is that the balance between gain and losses is achieved on significantly higher average powers as a result of the absence of output coupler losses in a steady-state system, which results in a reduced level of total losses. In other words (see Fig. 6), in the case of the same repetition rate in an all-normal ring cavity fiber laser with a cavity length of 2 km and

cavity-dumping laser with five periodical fiber cells of 400 m, the output energy of the second one will be higher with the lower pump power and broader stable generation area. Particularly, in Fig. 6, the case of $n = 1$ corresponds to the ring cavity fiber laser.

The results presented above show that the cavity dumping system may efficiently be used not only for active mode locking, but also for signal amplification. The advantages of the quasi-distributed gain are related to its potential ability to compensate for virtually unlimited losses on the output coupler, where the output energy principally depends on the losses between the two last active elements. For example, classical averaged equations of the Ginzburg–Landau type always give the strongly overestimated power values on stationary solutions, mainly because the compensated losses are also averaged. As for the cavity dumping systems, we have shown the efficiency of gain with a small number of active elements; on the contrary, the increase in the number of roundtrips of the periodic section leads to mode locking, but negatively affects the output signal power.

A fiber laser scheme with the quasi-distributed gain was considered. In order to maximize the average output power, the theoretical modeling was carried out for different numbers of active fiber cells. It has been shown that the average pulse power is decreased linearly, and energy approaches the constant with a significant growth in the number of active fiber cells. The optimal output pulse energy was also theoretically estimated. During the theoretical analysis, we have shown that the quasi-distributed gain allows to compensate for any cavity losses and, at the same time, enables to expand the stable pulse generation area by increasing the number of active fiber cells.

Funding. Russian Foundation for Basic Research (18-31-20027).

Disclosures. The authors declare no conflicts of interest.

REFERENCES

1. A. Ivanenko, S. Kobtsev, S. Smirnov, and A. Kemmer, *Opt. Express* **24**, 6650 (2016).
2. M. Malmström, Z. Yu, W. Margulis, O. Tarasenko, and F. Laurell, *Opt. Express* **17**, 17596 (2009).
3. A. F. Kornev, V. P. Pokrovskiy, S. V. Gagarskiy, Y. Y. Fomicheva, P. A. Gnatyuk, and A. S. Kovyarov, *Opt. Lett.* **43**, 3457 (2018).
4. L. Harris, M. Clark, P. Veitch, and D. Ottaway, *Opt. Lett.* **41**, 4309 (2016).
5. K. Krzempek, *Opt. Express* **23**, 30651 (2015).
6. S. Kaspar, M. Rattunde, T. Töpfer, U. Schwarz, C. Manz, K. Köhler, and J. Wagner, *Appl. Phys. Lett.* **101**, 141121 (2012).
7. L. McDonagh, R. Wallenstein, and R. Knappe, *Opt. Lett.* **31**, 3303 (2006).
8. Y. F. Ma, X. D. Li, X. Yu, R. P. Ren, R. G. Fan, J. B. Peng, X. R. Xu, Y. C. Bai, and R. Sun, *Appl. Opt.* **53**, 3081 (2014).
9. S. Smirnov, S. Kobtsev, A. Ivanenko, A. Kokhanovskiy, A. Kemmer, and M. Gervaziev, *Opt. Lett.* **42**, 1732 (2017).
10. O. V. Shtyrina, A. V. Ivanenko, I. A. Yarutkina, A. V. Kemmer, A. S. Skidin, S. M. Kobtsev, and M. P. Fedoruk, *J. Opt. Soc. Am. B* **34**, 227 (2017).
11. T. Pfeiffer and H. Büllow, *IEEE Photon. Technol. Lett.* **4**, 449 (1992).
12. E. Desurvire, *Erbium-Doped Fiber Amplifiers: Principles and Applications* (Wiley-Interscience, 1994).
13. I. A. Yarutkina, O. V. Shtyrina, A. Skidin, and M. P. Fedoruk, *Opt. Commun.* **342**, 26 (2015).
14. C. Barnard, P. Myslinski, J. Chrostowski, and M. Kavehrad, *IEEE J. Quantum Electron.* **30**, 1817 (1994).
15. S. K. Turitsyn, A. E. Bednyakova, M. P. Fedoruk, A. I. Latkin, A. A. Fotiadi, A. S. Kurkov, and E. Sholokhov, *Opt. Express* **19**, 8394 (2011).
16. J. L. Levy and R. C. Mayer, *Math. Comput. Model.* **12**, 919 (1989).

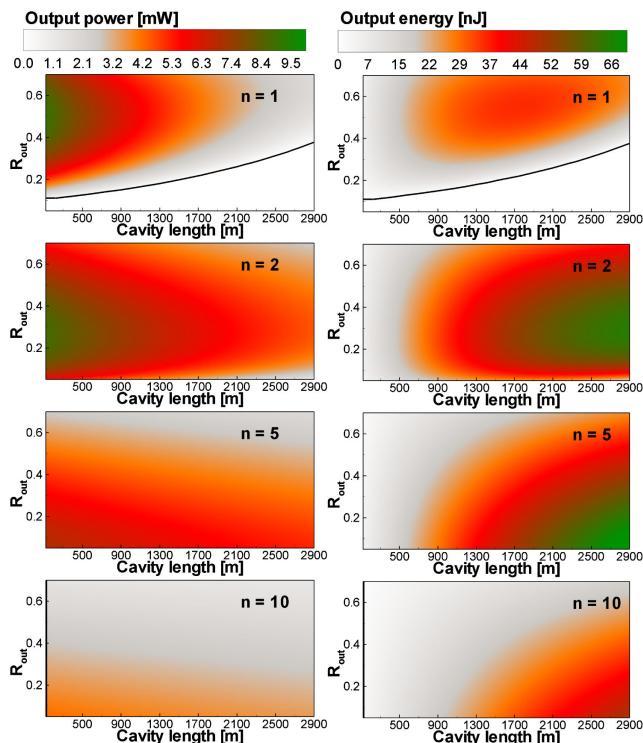


Fig. 6. Contour plots of output power and energy in (cavity length; R_{out}) plane for various numbers of fiber sections. The values of g and P_{sat} are defined using formulas for $P_{\text{pump}} = 0.7$ W and $L = 2.3$ m.